

# AN ACROSSWIND EQUIVALENT STATIC WIND LOAD MODEL FOR RECTANGULAR SHAPED TALL BUILDINGS

Chii-Ming Cheng<sup>1\*</sup>, Jenmu Wang<sup>1</sup>, Tzu-Ching Lai<sup>2</sup> and Ming-Shu Tsai<sup>2</sup>

<sup>1\*</sup>Department of Civil Engineering, Tamkang University, New Taipei City, Taiwan

<sup>2</sup>Wind Engineering Research Center, Tamkang University, New Taipei City, Taiwan

## Abstract

An acrosswind equivalent static wind load model for rectangular shaped tall buildings were proposed. In the proposed acrosswind force spectral model, specific physical meanings are given to the key parameters. In such a way, the empirical model is more in line with current understanding on building acrosswind loads, it can be improved by others with support of additional data. The lift coefficients and spectral estimates produced by the proposed model were compared with wind tunnel measurements with satisfactory results. A large number of prototype tall buildings were used to study the model performance in term of building overturning moment. For most cases, the base moment yielded by proposed ESWL model are either within 10% error bound or slightly conservative.

**Keywords:** Tall Building, Acrosswind Load, Wind Tunnel, Equivalent Static Wind Load.

## 1. INTRODUCTION

In typhoon-prone regions such as Taiwan, wind loads is an important factor for building design. It is well known that buildings are subjected to alongwind, acrosswind and torsional wind loads. For majority of the low-rise buildings, the alongwind load induced by approaching atmospheric turbulent boundary layer flow is the dominant wind load. The fundamental frame work for alongwind load was laid in 1960s by A.G. Davenport. The alongwind ESWL for building is now well-established and has been adopted by many wind codes in various forms. However, for many tall or super tall builidngs, acrosswind load bears equal or more weight than alongwind load in wind resistant design. The acrosswind load is primarily caused by vortex shedding phenomenon, which is sensitive to building shape and turbulence. Therefore, for the commonly seen rectangular shaped tall buildings, there exists no valid

theoretical or semi-analytical model to describe the acrosswind load. Current practices in various wind codes can be categorized into three types, they are: (i) acknowledge the importance of vortex induced acrosswind load and designate the response to building designer, such as ASCE7-10 (2010); (ii) directly adopting wind tunnel data, such as Australian/New Zealand Standard (2002); (iii) adopting empirical formulae derived from wind tunnel data, such as AIJ recommendations (2004). Empirical acrosswind load model, such as the one in AIJ-2004 or the mathematic formulae proposed by Liang et al., (2004), Tang et al (2010), parameters such as side ratio, aspect ratio, flow features are all or partially included. In those empirical formulae, in order to simulate the general shape of acrosswind force spectra, fractional mathematic expression were chosen to be the basic spectral form without clear physical meaning. Combining with proper lift force coefficient, these empirical models can produce reasonable acrosswind loads. However, these empirical models are difficult to adjust or improve, especially by a second party. This paper intends to build an empirical acrosswind equivalent static wind load model that holds sufficient physical meaning and can be further modified with additional experimental data even by others. Firstly, the wind tunnel produced aerodynamic data, which is the foundation of the empirical model will be briefly introduced. Then the basic concept and the mathematical formulation of the empirical model will be described. Accuracy of parameters will be examined. And then, tall buildings' base overturning moments produced by the proposed model will be compared with results based on wind tunnel data.

## 2. AERODYNAMIC DATA

### 2.1 Wind Tunnel Test

All wind tunnel tests were conducted in an open-circuit, suction type wind tunnel with test section of 17m in length, 2m in width and 1.5m in height. Three turbulent boundary layer flows, designated by *BL-A*, *BL-B*, *BL-C*, with power law index  $\alpha=0.32$ , 0.25, 0.15, were generated to represent wind profiles over urban, suburban and open country terrains, respectively. Acrylic pressure models and high speed electronic pressure scanner system were used in wind tunnel experiment. The geometry variations of the pressure models are: 11 sets of aspect ratio:  $H/\sqrt{BL}=2, 2.5, 3, 3.5, 4, 4.5, 5, 5.5, 6, 6.5, 7$ ; 13 sets of side ratios:  $L/B=1/5, 1/4, 1/3, 1/2.5, 1/2, 1/1.5, 1/1, 1.5/1, 2/1, 2.5/1, 3/1, 4/1, 5/1$ . All models have same cross-sectional area,  $(BL)=100\text{cm}^2$  i.e., same model height for a particular aspect ratio,  $H/\sqrt{BL}$ . For model with aspect ratio of  $H/\sqrt{BL}=7$ , 380 pressure taps were installed on 15 levels along the model height; and 9 levels, 230 pressure taps for the model with aspect ratio  $H/\sqrt{BL}=3$ . The sampling rate was 200Hz and the sample length was 287 seconds. During

AN ACROSSWIND EQUIVALENT STATIC  
WIND LOAD MODEL FOR RECTANGULAR  
SHAPED TALL BUILDINGS

model testing, Blockage ratio is less than 5%. Reynolds number for the upper half of the testing model was kept greater than  $4 \times 10^4$  which is higher than  $Re_{e,cr} \approx 2 \times 10^4$  required for Reynolds number similarity.

**2.1 Aero-Database for rectangular shaped buildings**

Shown in Figure 1 are the RMS base lift coefficients,  $C_L$  (defined in Eq.(4)), of building in three different flow fields. Since all models have same cross-sectional area and  $C_L$  was normalized with respect to breadth, B.  $C_L$  is primarily reflecting the side face area on which the acrosswind load asserted. Flow field condition and aspect ratio cast secondary effects. In urban terrain flow filed,  $BL-A$ ,  $C_L$  decreases with aspect ratio for all side ratio cases and increases with side ratio for all aspect ratio cases. In  $BL-B$  and  $BL-C$ ,  $C_L$  increases with increase of side ratio in general; however, for  $L/B=1.0 \sim 3.0$ ,  $C_L$  decreases with increase of side ratio due to reattachment phenomenon. For the model with smaller side ratio, lateral faces are subjected to bigger suctions due to complete vortex shedding, but the base lift force is reduced due to the relatively shorter side faces.

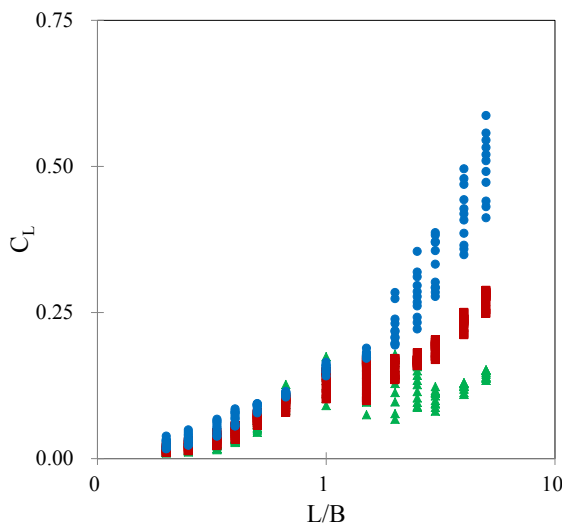


Figure 1. Variation of RMS base lift force coefficients.

● : BL-A , ■ : BL-B , ▲ : BL-C

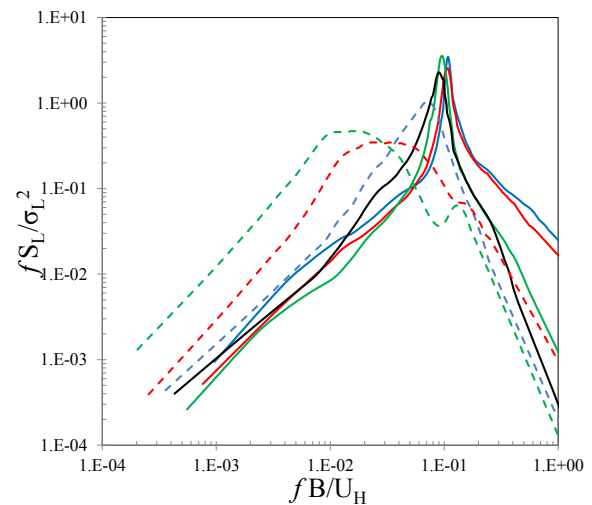


Figure 2. Reduced spectra of generalized acrosswind force of buildings with aspect ratio,

$H/VBL=6$ , in  $BL-B$ . — :  $L/B=0.2$  , - - :  $L/B=0.33$  , — :  $L/B=0.67$  , — :  $L/B=1$  , - - :  $L/B=1.5$  , - - :  $L/B=3$  , - - :  $L/B=5$

The effect of side ratio,  $L/B$ , on reduced generalized acrosswind force spectra in suburban flow field,  $BL-B$ , is shown in Figure 2. The spectra of various side ratio can be categorized into two groups. For models with side ratio less than 1.0, the lift spectra show significantly high energy contents near the Strouhal frequency of  $fB/U_H \approx 0.1$ . For  $L/B > 1$ , spectral peak induced by vortex shedding gradually reducing and move towards lower frequency as reattachment becomes more obvious and

consequently narrowing the separation wake. At the same time, a second spectral peak induced by reattachment and rear end separation gradually emerges especially for large aspect ratio and in open terrain flow field, *BL-C*. For buildings with low aspect ratio, end effects and high turbulence intensity tend to obscure spectral peaks induced by vortex shedding and reattachment. It also can be observed that higher turbulence intensity will increase the spectral bandwidth, thus, increase the spectral estimates in higher frequency region where buildings natural frequencies are.

### 3. ACROSSWIND ESWL MODEL

Assessment of the human comfort under wind induced motion is an important wind resistant design consideration. For most of the tall buildings, building acceleration is dominated by the resonant part. It is, therefore, important for structural engineers to be able to extract the resonant part of the design wind load. For this purpose, the ESWL can be arranged in the following form (Holmes, 2001):

$$W_L(z) = G_B(z)F_{L,B}(z) + G_R(z)F_{L,R}(z) \quad (1)$$

where  $G_B(z)$  and  $G_R(z)$  are given by:

$$G_B(z) = \frac{g_B F_{L,B}(z)}{\left(g_B^2 F_{L,B}^2(z) + g_R^2 F_{L,R}^2(z)\right)^{1/2}} \quad (2)$$

$$G_R(z) = \frac{g_R F_{L,R}(z)}{\left(g_B^2 F_{L,B}^2(z) + g_R^2 F_{L,R}^2(z)\right)^{1/2}}$$

The background part of ESWL,  $F_{L,B}(z)$  is given by:

$$F_{L,B}(z) = \rho U_H^2 C_L B \quad (3)$$

In which,  $C_L$  is the overturning moment based spatial averaged fluctuation lift force coefficient, and given by:

$$C_L = \sigma_L / \frac{1}{2} \rho U_H^2 B H^2 \quad (4)$$

$\sigma_L$  is the RMS of wind tunnel measured base moment. The resonant part of the equivalent static load is assumed to have same distribution as the inertia force. Assuming the building mass is uniformly distributed along building height and the fundamental mode shape assumed to have the form of  $\varphi(z) = (z/H)^\beta$ . The resonant part

AN ACROSSWIND EQUIVALENT STATIC  
WIND LOAD MODEL FOR RECTANGULAR  
SHAPED TALL BUILDINGS  
of ESWL,  $F_{L,R}(z)$  is given by:

$$F_{L,R}(z) = (2\beta + 1) \frac{1}{H} \left( \frac{z}{H} \right)^\beta \left[ \frac{\pi f_0 S_L(f_0)}{4\xi} \right]^{1/2} \quad (5)$$

#### 4. EMPIRICAL FORMULAE FOR LIFT COEFFICIENT AND FORCE SPECTRA

The lift coefficient used in this article,  $C_L$ , is an overturning moment based spatial averaged force coefficient. In other words, the base moment calculated by adopting  $F_{L,B}(z)$  along building height would be same as the wind tunnel results. Generally speaking, lift coefficient is primarily a function of building side ratio,  $L/B$ . Building aspect ratio and terrain condition cast secondary effects. This paper proposes the following form for  $C_L$ :

$$C_L = \ell_1 \left( \frac{L}{B} \right)^3 + \ell_2 \left( \frac{L}{B} \right)^2 + \ell_3 \left( \frac{L}{B} \right) + \ell_4 \left( \frac{L}{B} \right)^{\ell_5} \left( \frac{H}{\sqrt{BL}} \right)^{\ell_6} \quad (6)$$

The values for  $\ell_i$  in three terrain categories are listed in Table 1.

Table 1. Coefficients for  $C_L$  in Eq. (6)

	$\ell_1$	$\ell_2$	$\ell_3$	$\ell_4$	$\ell_5$	$\ell_6$
BL-A	0.0047	-0.03	0.19	-0.006	1.7	0.67
BL-B	0.0106	-0.09	0.25	-0.04	0.13	-0.01
BL-C	0.0144	-0.13	0.39	-0.018	0.53	-0.13

Buildings' acrosswind force are combined results of vortex shedding, lateral turbulence and end effects. For rectangular shaped tall buildings, the acrosswind force spectra are complex function of several variables:  $L/B$ ,  $H/\sqrt{BL}$ , wind speed gradient and turbulence intensity. Although it is unrealistic to derive an analytical model that fully reflects the nature of acrosswind phenomenon. This paper intends to develop an empirical model with parameters containing clear physical meanings. Vickery & Clark (1972) based on the assumption that, in turbulent flow, vortex shedding frequency has nature of Gaussian process and proposed the famous lift force spectrum for circular cylinder:

$$\frac{fS_L(f)}{\sigma_L^2} = \frac{(f/f_s)}{\sqrt{\pi B_e}} \exp \left[ - \left( \frac{1 - (f/f_s)}{B_e} \right)^2 \right] \quad (7)$$

In which,  $f_s$  is vortex shedding frequency and  $B_e$  is spectral bandwidth. In later years, similar spectral formulations had been used for rectangular buildings with little success. That is because lateral turbulence and reattach phenomenon play important role in the acrosswind loads of rectangular shaped tall buildings and cannot be ignored as in the case of circular cylinder. Based on the aforementioned observations, this article proposes the following empirical model for the generalized acrosswind force spectra of rectangular shaped tall buildings:

$$\tilde{S}_L(f) = \frac{fS_L(f)}{\sigma_L^2} = \sum_{i=0}^2 S_{Li}(f) \quad (8)$$

$L/B \leq 2, \quad i = 0, 1; \quad L/B > 2, \quad i = 0, 1, 2$

In which,  $\sigma_L'$  is the RMS of the generalized lift force spectrum. The first term,  $S_{L0}(f)$ , represents the spectral contribution from lateral turbulence and the end effects from building top and bottom. The second term,  $S_{L1}(f)$ , represents contribution from vortex shedding process. The third term,  $S_{L2}(f)$ , represents contribution from the reattachment phenomenon.  $S_{L0}(f)$  has the following form:

$$S_{L0}(f) = A_0 \chi_R(f) S_V(f) \quad (9)$$

$$A_0 = C_0 * \left(\frac{L}{B}\right)^{-0.8} * \left(\frac{H}{\sqrt{BL}}\right)^{0.76} \quad (10)$$

In which,  $C_0=0.36, 0.30, 1.2$  for terrain  $A, B$  and  $C$ , respectively.  $S_V(f)$  is reduced lateral turbulence spectrum and  $\chi_R(f)$  is an quasi-steady assumption based aerodynamic admittance function originally derived for the longitudinal turbulence effects on building alongwind force.  $S_{L1}(f)$  and  $S_{L2}(f)$  have the general form of:

$$S_{Li}(f) = A_i \exp \left[ - \left| \frac{1 - f/f_{si}}{Be_i} \right|^{z_i} \right], \quad i = 1, 2 \quad (11)$$

In Which,  $A_1$  and  $A_2$  are magnitude of spectral estimates at the center frequencies of vortex shedding and reattachment, respectively. Both  $A_1$  and  $A_2$  are functions of building side ratio, aspect ratio and terrain condition. Coefficients  $C_1$  to  $C_4$  in Eq. (11) and listed in Table 2 have different values for three terrain categories.

AN ACROSSWIND EQUIVALENT STATIC  
WIND LOAD MODEL FOR RECTANGULAR  
SHAPED TALL BUILDINGS

$$A_1 = C_1 * \left(\frac{L}{B}\right)^{C_2} * \left(\frac{H}{\sqrt{BL}}\right)^{C_3}$$

$$A_2 = C_4 * \left(\frac{L}{B}\right)^{0.11} * \left(\frac{H}{\sqrt{BL}}\right)^{0.2}$$
(12)

$f_{s1}$  and  $f_{s2}$  are center frequencies of vortex shedding and reattachment phenomenon, respectively. Vortex shedding frequency,  $f_{s1}$ , is mainly a function of building side ratio,  $L/B$ , only. Center frequencies for reattachment, which is valid only for  $L/B > 2$ , is a function of aspect ratio as shown in Eq. (12).

$$f_{s1} = -0.03 * \left(\frac{L}{B}\right)^{0.7} + 0.12$$

$$f_{s2} = -0.01 * \left(\frac{H}{\sqrt{BL}}\right)^{0.7} + 0.17$$
(13)

$B_{e1}$  and  $B_{e2}$  are spectral bandwidth near vortex shedding frequency,  $f_{s1}$ , and reattachment center frequency,  $f_{s2}$ . At each terrain category,  $B_{e1}$  is function of side ratio,  $L/B$ , and longitudinal turbulent intensity,  $I_u$ , at two-third of building height.  $B_{e2}$  is a function of side ratio only. Experimental data reveals that spectral bandwidth of vortex shedding,  $B_{e1}$ , varies significantly between short rectangular shape,  $L/B < 1$ , and long rectangular shape,  $L/B > 1$ . Therefore, coefficient  $C_5$  has two sets of values for different side ratio as listed in table 3.

$$B_{e1} = C_5 * \left(\frac{L}{B}\right)^{C_6} (I_u)^{C_7}$$

$$B_{e2} = C_8 * \left(\frac{L}{B}\right)^{0.01}$$
(14)

$\gamma_i$  represents the rate of energy decay as frequency away from the spectral peaks, i.e.,  $f_{s1}$  and  $f_{s2}$ . Unlike a constant value,  $\gamma=2$  for circular cylinder, values of  $\gamma_i$  decrease in a rather complex manner. When contribution from vortex shedding decay rapidly as frequency distanced from the vortex shedding/reattachment frequencies,  $f_{si}$ , the contributions from lateral turbulence and end effects would compensate the energy loss and slow down the rate of energy decay. Let

$$f_i^* = \frac{|1 - f / f_{si}|}{B_{e_i}}, \quad i = 1, 2$$

$$f_i^* \leq \tilde{f}, \quad \gamma_i = 2$$

$$f_i^* > \tilde{f}, \quad \gamma_i = 2 - C_9 * \left(\frac{L}{B}\right)^{C_{10}} \left(\frac{H}{\sqrt{BL}}\right)^{C_{11}} \left(\frac{\tilde{f}}{f_i^*} - 1\right)^2 \quad (15)$$

In which,  $\tilde{f} = 0.4$  for terrain A and B,  $\tilde{f} = 0.6$  for terrain C.

Table 2. Empirical coefficients in spectral models

Terrain	$C_1$	$C_2$	$C_3$	$C_4$	$C_6$
A	0.22	-0.73	0.6	0.015	0.4
B	0.19	-0.97	0.83	0.045	0.68
C	0.34	-0.97	0.83	0.15	1.06
Terrain	$C_7$	$C_8$	$C_9$	$C_{10}$	$C_{11}$
A	1.71	0.59	1.58	-0.08	-0.05
B	1.57	0.45	1.58	-0.08	-0.05
C	0.62	0.38	1.67	0	-0.12

Table 3. Values for  $C_5$  in Eq. (14)

Terrain	$0.2 \leq L/B < 1.0$	$1.0 \leq L/B \leq 5.0$
A	6.28	11
B	6.86	9
C	1.38	1

### 5. ACCURACY OF EMPIRICAL MODELS AND PARAMETERS

Shown in Figure 3 are comparison of lift coefficient between proposed model, Eq. (6), and wind tunnel measurements. Figure 3 shows that, except small number cases of under-estimation in low fields  $BL-B$  and  $BL-C$ , Eq. (6) predicts satisfactory values for  $C_L$  within 10% error marked by the two dash lines.

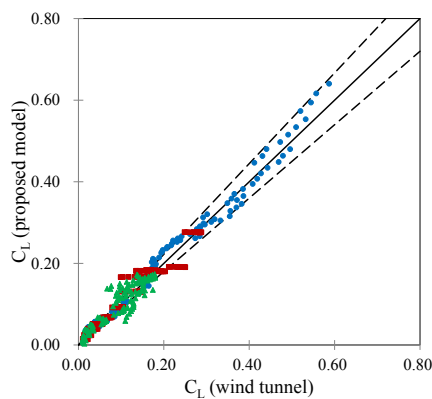


Figure 3. Comparison of lift coefficient  $C_L$  in Eq. (5). ●: BL-A, ■: BL-B, ▲:

Comparison of center frequency of vortex shedding,  $f_{sl}$ , is plotted in Figure 4. Wind tunnel data reveals that vortex shedding frequency,  $f_{sl}$ , is primarily a function of side ratio,  $L/B$ , only. The empirical formula for  $f_{sl}$  performs quite well. Except over-estimated for some cases in flow field  $BL-C$ , the values given by empirical formula agree well with



AN ACROSSWIND EQUIVALENT STATIC  
WIND LOAD MODEL FOR RECTANGULAR  
SHAPED TALL BUILDINGS

wind tunnel data. Comparisons of vortex shedding spectral bandwidth,  $B_{e1}$ , are plotted in Figure 5. The spectral bandwidth of experimental data were estimated as the normalized frequency interval at half-power points with respect to  $f_{s1}$ . For  $L/B \leq 0.67$ ,  $B_{e1}$  is primarily a function of side ratio; turbulence has secondary effect on it. For  $L/B \geq 1.0$ , aspect ratio also casts significant effect on  $B_{e1}$ . Values of  $B_{e1}$  obtained from wind tunnel data show more scattering than  $f_{s1}$ . It is quite natural that the comparison of  $B_{e1}$  exhibits larger error than  $f_{s1}$ . For many cases of building geometry, both the center frequency and bandwidth of reattachment,  $f_{s2}$  &  $B_{e2}$ , in the third spectral term,  $S_{L2}(f)$ , are difficult to estimate from wind tunnel data and show more randomness than  $f_{s1}$  and  $B_{e1}$ . The performance of these empirical formulae are less satisfactory.

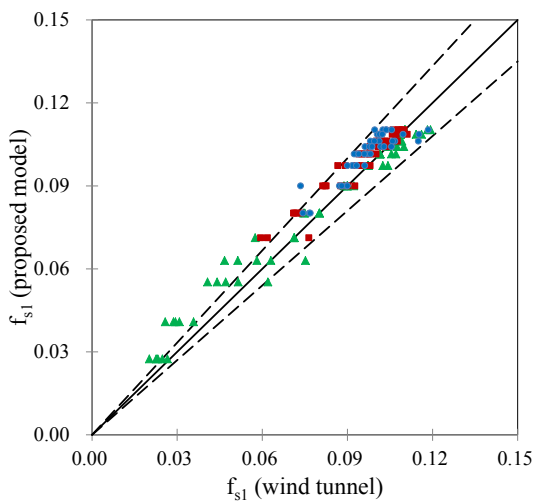


Figure 4. Comparison of parameter  $f_{s1}$  in Eq. (12). ●: BL-A, ■: BL-B, ▲: BL-C

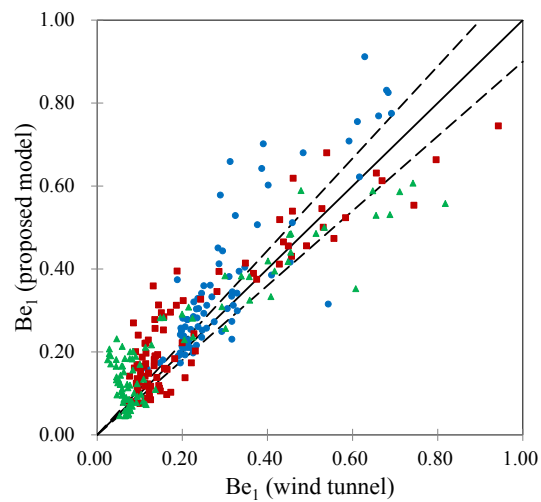


Figure 5. Comparison of parameter  $B_{e1}$  in Eq. (13). ●: BL-A, ■: BL-B, ▲: BL-C

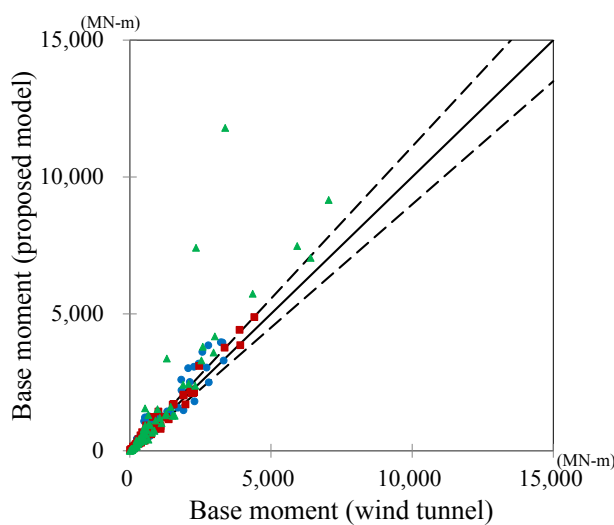


Figure 6. Comparisons of prototype buildings' base moments. ●: BL-A, ■: BL-B, ▲: BL-C

## 6. CASE STUDY

A group of prototype tall buildings were chosen to study the design wind loads. Assuming all buildings have the identical cross-sectional area,  $(BL)=900 \text{ m}^2$ , and same story height,  $h=3.6 \text{ m}$ . For example, building with side ratio  $L/B=1/3$  and aspect ratio  $H/\sqrt{BL}=6$  would be a 50-story building with 52m in breadth, 17.3m in depth and 180m in height. The natural periods were

assuming to be one-tenth of the story number in seconds. Damping ratio to be 0.01 for all buildings. Total of 78 prototype tall buildings were used, in each three terrain categories. The acrosswind design wind loads were estimated and henceforward to calculate the overturning moments.

The comparison of buildings overturning moment calculated from proposed acrosswind ESWL model and the value based on wind tunnel data is plotted in Figure 6. The proposed ESWL model performed quite well for most cases, i.e., the results are either within 10% error bound or slightly conservative. However, there are a few cases where the ESWL model yields over-conservative results when buildings are located in open country terrain category, i.e., flow field *BL-C*.

## 7. CONCLUSIONS

In this article, an acrosswind equivalent static wind load model for rectangular shaped tall buildings were proposed based on wind tunnel data. In the proposed acrosswind force spectral model, specific physical meanings are given to the key parameters. In such a way, not only the empirical model is more in line with current understanding on building acrosswind loads, this model can be improved by others with support of additional data. The lift coefficients and spectral estimates produced by the proposed model were compared with wind tunnel measurements with satisfactory results. On the final stage, a large number of prototype tall buildings were used to study the model performance in term of building overturning moment. For most cases, the base moment yielded by proposed ESWL model are either within 10% error bound or slightly conservative. There indeed have a few cases where the ESWL model are over-conservative. Authors noticed that the aerodynamic admittance function,  $\chi_R(f)$ , used in the first term of spectra model calls for further investigation to improve the accuracy of the proposed model.

## 8. REFERENCES

- [1] DAVENPORT A G. 1968. The dependence of wind load upon meteorological parameters. Proceedings of the international research seminar on wind effects on buildings and structures. Toronto, Canada. 19-82.
- [2] VICKERY B J, CLARK A W. 1972. Lift or crosswind response of slender stack[J]. ASCE Journal of Structural Engineering. 98(1).
- [3] HOLMES J D. 2001. Wind Loading of Structures[M]. London. Spon Press.
- [4] AS/NZ1170.2:2002. Australian/New Zealand Standard on Wind Actions.
- [5] LIANG S, LIU S, LI Q S, ZHANG L, GU M. 2002. Mathematical model of acrosswind dynamic loads on rectangular tall buildings[J]. Journal of Wind Engineering and

AN ACROSSWIND EQUIVALENT STATIC  
WIND LOAD MODEL FOR RECTANGULAR  
SHAPED TALL BUILDINGS

Industrial Aerodynamics. (90):1757–1770.

- [6] AIJ-2004. Architectural Institute of Japan. Recommendations for Loads on Buildings.
- [7] ASCE7-10, 2010. Minimum design loads for buildings and other structures.
- [8] TANG Y, GU M, QUAN Y. 2010. Fluctuating force of across-wind acting on rectangular super-tall buildings, Part II: Mathematical model[J]. Journal of Vibration and Shock. 29(6). (in Chinese)